Science of the Total Environment 814 (2022) 152767

Contents lists available at ScienceDirect

Science of the Total Environment

journal homepage: www.elsevier.com/locate/scitotenv

Influence of Fe(III) source, light quality, photon flux and presence of oxygen on photoreduction of Fe(III)-organic complexes – Implications for light-influenced coastal freshwater and marine sediments

Ulf Lueder [a,*], Bo Barker Jørgensen [b], Markus Maisch [a], Caroline Schmidt [a,c], Andreas Kappler [a,b,d]

[a] Geomicrobiology Group, Center for Applied Geoscience (ZAG), University of Tuebingen, Schnarrenbergstrasse 94-96, D-72076 Tuebingen, Germany
[b] Section for Microbiology, Department of Biology, Aarhus University, Ny Munkegade 114, 8000 Aarhus, Denmark
[c] Tuebingen AI Center, University of Tuebingen, Maria-von-Linden-Strasse 6, D-72076 Tuebingen, Germany
[d] Cluster of Excellence: EXC 2124: Controlling Microbes to Fight Infection, Tübingen, Germany

HIGHLIGHTS

- Organic complexation controls Fe(III) photoreduction and Fe(II) and H_2O_2 turnover
- Same extent and rate of photoreduction with biogenic and abiogenic Fe(III) minerals
- Organic ligand availability leads to steady-state micromolar Fe(II) in sediments.

GRAPHICAL ABSTRACT

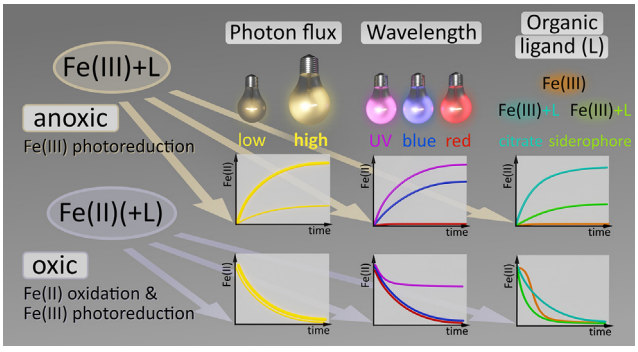

ARTICLE INFO

Article history:
Received 14 October 2021
Received in revised form 30 November 2021
Accepted 25 December 2021
Available online 1 January 2022

Editor: Jay Gan

Keywords:
Iron(III) photoreduction
Iron(II) oxidation
Reactive oxygen species
Light
Organic complexation
Redox reactions

ABSTRACT

Iron(III) photoreduction is an important source of Fe(II) in illuminated aquatic and sedimentary environments. Under oxic conditions, the Fe(II) can be re-oxidized by oxygen (O_2) forming reactive O-species such as hydrogen peroxide (H_2O_2) which further react with Fe(II) thus enhancing Fe(II) oxidation rates. However, it is unknown by aquatic sediments how the parameters wavelength of radiation, photon flux, origin of Fe(III) source and presence or absence of O_2 influence the extent of Fe(II) and H_2O_2 turnover. We studied this using batch experiments with different Fe(III)-organic complexes mimicking sedimentary conditions. We found that wavelengths <500 nm are necessary to initiate Fe(III) photoreduction and that the photon flux, wavelength and identity of Fe(III)-complexing organic acids control the kinetics of Fe(III) photoreduction. The formation of photo-susceptible Fe(III)-organic complexes did not depend on whether the Fe(III) source was biogenically produced, poorly-crystalline Fe(III) oxyhydroxides or chemically synthesized ferrihydrite. Oxic conditions caused chemical re-oxidation of Fe(II) and accumulation of H_2O_2. The photon flux, wavelength and availability of Fe(III)-complexing organic molecules are critical for the balance between concurrent Fe(III) photoreduction and abiotic Fe(II) oxidation and may even lead to a steady-state concentration of Fe(II) in the micromolar range. These results help understand and predict Fe(III) photoreduction dynamics and in-situ formation of Fe(II) in oxic or anoxic, illuminated and organic-rich environments.

* Corresponding author at: Geomicrobiology, Center for Applied Geoscience, University of Tuebingen, Schnarrenbergstrasse 94-96, D-72076 Tuebingen, Germany.
E-mail address: lueder.ulf@gmail.com (U. Lueder).

http://dx.doi.org/10.1016/j.scitotenv.2021.152767

1. Introduction

1.1. Iron redox cycling in the environment

Iron (Fe) is widely distributed in the environment, where it occurs as ferrous iron (Fe(II)) and ferric iron (Fe(III)). While iron is commonly found at micromolar concentrations of Fe(II) dissolved in porewater of sediments (Canfield, 1989; Schaedler et al., 2018; Thamdrup et al., 1994), concentrations in oxic water columns are usually in the nano- or picomolar range (Boyd and Ellwood, 2010; Emmenegger et al., 2001; King and Barbeau, 2011). Iron is cycled between the two redox states by different biotic and abiotic processes (Kappler et al., 2021). One important redox process in illuminated environments is Fe(III) photoreduction, during which mainly organically complexed Fe(III) (dissolved complexes or organic molecules adsorbed on Fe(III) (oxyhydr)oxide mineral surfaces) (Barbeau, 2006; Borer et al., 2009a; Sulzberger et al., 1989; Waite and Morel, 1984a) is reduced to Fe(II) by either direct ligand-to-metal charge transfer (LMCT) or by photochemically produced radicals such as superoxide ($O_2^{\cdot-}$) (Barbeau, 2006; Garg et al., 2020; Kuma et al., 1995; Lee et al., 2017; Miller et al., 1995; Rose and Waite, 2005; Xing et al., 2019). The complexing ligand is oxidized, eventually to carbon dioxide (Abrahamson et al., 1994). Fe(III) photoreduction is an important process for providing potentially bioavailable dissolved Fe(II) (Johnson et al., 1994; Miller and Kester, 1994), changing prevalent Fe(II) fluxes in sediment (Lueder et al., 2020a). However, Fe(II) gets rapidly chemically oxidized, e.g. by oxygen (O_2) (Davison and Seed, 1983; Millero et al., 1987). During oxidation of Fe(II) by O_2, reactive oxygen species (ROS) such as hydrogen peroxide (H_2O_2) form, which in turn can oxidize Fe(II) and enhance overall Fe(II) oxidation rates (Kanzaki and Murakami, 2013; King et al., 1995; Miller et al., 1995; Rose and Waite, 2002). In the presence of O_2, ROS can also form by light-induced reactions of dissolved organic matter (DOM) (Garg et al., 2011; Li et al., 2015; Mostafa and Rosario-Ortiz, 2013; Page et al., 2014; Scully et al., 1996; Zhang et al., 2014). The highly reactive oxygen species impact the biogeochemical iron cycle (Hansel et al., 2015). In oxic, illuminated environments, formation of Fe(II) by Fe(III) photoreduction and Fe(II) depletion by reaction with O_2 and produced ROS or organic radicals (Garg et al., 2018) are therefore in competition and impact the redox state of Fe.

1.2. Consequences of organic complexation for iron redox reactions

Organic complexation, e.g. by microbially excreted siderophores, organic acids or plant-released organic exudates, strongly increase the solubility of Fe(III) (Kraemer, 2004; Kuma et al., 1996; Marschner et al., 1986) and is crucial for Fe(III) photoreduction at circumneutral pH (King et al., 1993). Diverse organic ligands are ubiquitously found in the environment (Fox and Comerford, 1990; Gledhill and Buck, 2012; Hopwood et al., 2015; Luther et al., 1996) and complexation can either slow down or accelerate Fe(II) oxidation depending on the kind of organic ligand (Miles and Brezonik, 1981; Santana-Casiano et al., 2000; Theis and Singer, 1974). Therefore, it is difficult to predict how much the identity and availability of organic ligands determine the efficiency, i.e. the kinetics and extent, of Fe(III) photoreduction. Citrate is an α-hydroxy tricarboxylic acid that easily forms complexes with Fe(III) and it is, besides other carboxylic acids, commonly found in natural environments (Fox and Comerford, 1990; Krishnamurti and Huang, 1991; Zhang and Yuan, 2017). Different siderophores are excreted for Fe acquisition (Saha et al., 2013) by plants, fungi and many microorganisms, including *Marinobacter* spp. (Barbeau et al., 2002), which are globally found in seawater and sediment (Gorshkova et al., 2003; Raddadi et al., 2017; Singer et al., 2011), and *Geobacter sulfurreducens*, which is an abundant Fe(III)-reducer and produces siderophores under Fe-limiting conditions (Caccavo et al., 1994).

1.3. Knowledge gaps and motivation for the study

Besides the unclear impact of availability and identity of organic ligands on light-induced Fe(II) formation in aquatic sediments, it is also unknown if biogenically formed Fe(III) minerals and abiotically formed ferrihydrite differ in organic complexation and Fe(III) photoreduction efficiency. It has previously not been determined if biogenically or chemically formed Fe(III) (oxyhydr)oxides show different reactivity towards the formation of photolabile Fe(III)-organic complexes and subsequent Fe(III) photoreduction. The impact of parameters that influence the rates and extent of Fe(III) photoreduction and consequently the fate and redox state of Fe in the environment, such as light intensity (photon flux), light energy (wavelength) or organic complexation have indeed been investigated for pico- or nanomolar concentrations of Fe in surface waters or the ocean (Borer et al., 2009a, 2009b; Emmenegger et al., 2001; Faust and Zepp, 1993; Garg et al., 2018; Kuma et al., 1995; Miller et al., 1995; Rijkenberg et al., 2005, 2006; Voelker et al., 1997; Waite et al., 1995) but are poorly described for environments with high Fe content, such as found in sediments (Canfield, 1989; Schaedler et al., 2018; Thamdrup et al., 1994). It is therefore unknown if data obtained in open water bodies can be used to Fe redox kinetics in sedimentary systems. Also, as illuminated sediments often fluctuate between oxic and anoxic conditions, it is important to experimentally distinguish Fe(III) photoreduction and Fe(II) oxidation to understand the relevance of each of these processes in the environment. Therefore, in order to systematically determine the parameters that influence Fe(III) photoreduction at micromolar concentrations in the presence of potential organic ligands, we performed a combined study of the influence of Fe(III) source, light intensity, wavelength and organic ligands on photoreduction of biogenically and chemically synthesized Fe(III) minerals at concentrations relevant for freshwater and marine sediments. The aims of this study are: i) to quantify the kinetics of Fe(II) formation of different Fe(III)-organic complexes during illumination at different light conditions in anoxic conditions over time, ii) to identify the reactivity of biogenically formed Fe(III) minerals compared to abiotic ferrihydrite, iii) to follow Fe(II) and H_2O_2 dynamics over time at different illumination conditions when O_2 is present, and iv) to determine the parameters that ultimately control the prevalent redox state of Fe under conditions found in light-influenced sediments.

2. Materials and methods

2.1. Fe(III) mineral synthesis, analysis, and isolation of organic ligands

The procedures for ferrihydrite synthesis, preparation of biogenically formed Fe(III) minerals, and the isolation of siderophores and organic ligands are described in the Supporting Information.

2.2. Experimental setup

In order to determine kinetics and extent of Fe(III) photoreduction under conditions relevant for sediments, different mixtures of Fe(III) minerals and organic ligands were incubated in anoxic 10 mM HCO_3^- buffered MilliQ water adjusted to pH 7 at different light intensities and wavelengths (Table S1 and Fig. S1) or in dark while Fe(II) development was quantified over time. Two different UV light sources were used with different maximum wavelength peaks at 395 nm and 365 nm, respectively (Table S2 and Fig. S1). They are subsequently called “UV 365 nm” and “UV 395 nm” light despite their spectra also contain other wavelengths as well.

Ferrihydrite and citrate or biogenically formed Fe(III) minerals and citrate were added to a final concentration of 300 μM each to the buffered anoxic MilliQ. Supernatants containing microbially-derived siderophores were used as directly prepared from the cultures after sterile-filtering and added in a volumetric ratio of 1:4 to buffered anoxic MilliQ to avoid potential influence of high ionic strength to Fe(II) formation. Illumination conditions (Table S1) were adjusted using a calibrated UV-VIS optical fiber (QP400–2-UV-BX, Ocean Insight, Germany) connected to a spectrometer (USB4000, Ocean Insight, Germany). The suspensions were continuously illuminated with different light-emitting diode lamps and Lee filters (Table S2 and Fig. S1). Anoxic suspensions were sampled daily for 4 days and Fe(II) was quantified.

To determine the simultaneous effect of chemical Fe(II) oxidation by O_2 and Fe(III) photoreduction on the development of Fe(II) concentrations, the headspace of anoxic 10 mM HCO_3^- buffered MilliQ (pH 7) with 300 μM $FeCl_2$ or 300 μM abiogenic ferrihydrite and organic ligands was aerated with air (30% of total headspace volume) and incubated at different illumination conditions (Table S1). Organic ligands were either Na-citrate (300 μM or 3 mM) or siderophores from *Marinobacter* sp. TT1 (Gutierrez et al., 2013) (added in a volumetric ratio of 1:4 to 10 mM HCO_3^- buffered MilliQ, pH 7). Before aeration, anoxic suspensions containing ferrihydrite and the respective organic ligands were incubated in UV 365 nm light for 3 days to photochemically form Fe(II). Oxic suspensions were sampled just before and 0.5, 1, 1.5, 2, 3, 4, 6 and 8 h after aeration and Fe(II) and H_2O_2 were quantified.

2.3. Fe and H_2O_2 quantification

Fe(II) and total Fe concentrations were spectrophotometrically determined by the ferrozine assay (Stookey, 1970). H_2O_2 was spectrophotometrically quantified with leuco crystal violet (Cohn et al., 2005; Mottola et al., 1970). Briefly, the sample was added to EDTA (final concentration 10 mM) to chelate dissolved Fe(II) and stabilize H_2O_2. Then, 100 mM KH_2PO_4, 41 μM leuco crystal violet and 1 μg (0.18 units) horseradish peroxidase were added to the sample and absorbance was measured at 592 nm in triplicates after 1 day. Calibration of H_2O_2 was performed in an additional setup on another day. However, as the method is highly sensitive to media composition, subtracting the calibration blank from low absorbance values of samples eventually led to slightly negative concentrations. Instead, lowest absorbance values for H_2O_2 of each experimental setup were used as respective blanks and subtracted to quantify H_2O_2. Concentrations below 1 μM should therefore be treated with care.

2.4. Rate calculations

Fe(III) photoreduction rate constants k for illuminated anoxic suspensions as well as net rates of reaction (i.e. Fe(II) oxidation) between different sampling intervals were determined as described in the Supporting Information.

3. Results and discussion

3.1. Influence of photon flux and light wavelength on Fe(III) photoreduction

In order to determine how photon flux and light wavelength influence Fe(III) photoreduction, we performed different incubation experiments. We found that the higher the photon flux of VIS light, the faster Fe(II) was formed from different Fe(III)-organic complexes by Fe(III) photoreduction, while no Fe(II) formation was found during dark incubation (Fig. 1 A, C,E). This confirms the dependence of light-induced Fe(II) formation on light intensity, i.e. photon flux (Kuma et al., 1995; Waite et al., 1995), but we could show by comparing Fe(III) reduction rate constants derived from light-induced reduction of different Fe(III)-organic complexes that illumination with a 6–8 (medium to high photon flux) or 120–130 times higher (low to high photon flux) VIS photon flux does not lead to changes of Fe(III) reduction rates in the same order of magnitude (Fig. 2). We saw that photon fluxes of 150–200 (medium photon flux) and 1200–1300 μmol photons m^{-2} s^{-1} (high photon flux) even led to similar Fe(II) production dynamics (Fig. 1 C) indicating light saturation of the process. Due to the absence of O_2, Fe(III) photoreduction in anoxic conditions is most probably driven by direct LMCT reactions by which absorption of photons leads to an electron transfer from the organic ligand to complexed Fe(III) (Kuma et al., 1995; Waite and Morel, 1984b) and explains the dependence of Fe(II) formation on photon flux. Our results indicate that above a certain photon flux threshold, Fe(II) formation kinetics is not directly controlled by photon flux but rather by other factors such as the identity, availability and concentration of photo-susceptible Fe(III)-organic complexes. Illumination of certain Fe(III)-organic complexes such as Fe(III)-citrate with a low photon flux of VIS light (10 μmol photons m^{-2} s^{-1}) can lead to significant Fe(II) formation in the micromolar range within hours (Fig. 1 A), thus highlighting the importance of Fe(III) photoreduction as Fe(II) source even in environments with low light availability, such as in sediments (Kühl et al., 1994; Lueder et al., 2020a, 2020c). Illumination of Fe(III)-organic complexes with light containing only wavelengths above 500 nm (green or red light) did not show Fe(II) formation (Fig. 1 B,D,F); i.e. the energy of the photons was not sufficient to induce a LMCT from the organic ligand to the complexed Fe(III), which is consistent with previous studies (Borer et al., 2009b; Rich and Morel, 1990; Weller et al., 2013). Illumination with light of shorter wavelengths, but with similar photon fluxes, showed a clear trend of shorter wavelengths to cause faster Fe(III) photoreduction (Pehkonen et al., 1993) (UV 365 nm light > UV 395 nm light > blue light) (Fig. 1 B,D,F) and consequently higher Fe(III) photoreduction rates (Fig. 2).

Similar observations as ours of the dependence of Fe(II) production on light intensity and wavelength in the case of micromolar concentrations of abiotic ferrihydrite or biogenic Fe(III) oxyhydroxide minerals in anoxic conditions were made in Fe(III) photoreduction studies using nanomolar Fe concentrations in oxic surface waters. Waite et al. (1995), for instance, found that Fe(II) concentrations in northern Australian shelf waters depend on light intensity, following diel variations in light intensity. Others pointed out the effectiveness and contribution of UV light to the overall Fe(III) photoreduction in Arctic waters or in the Southern Ocean (Laglera and Van Den Berg, 2007; Rijkenberg et al., 2004, 2005). Rijkenberg et al. (2004) formulated a function for wavelength-dependent Fe(II) production to quantify the effectiveness of different wavelengths for Fe(III) photoreduction in Antarctic seawater.

3.2. Effect of organic ligand and Fe(III) source for light-induced Fe(II) formation

Organic complexation and the identity of organic ligand, or more precisely the type of its Fe-complexing functional groups, affect the rate of Fe(III) photoreduction at circumneutral pH (Barbeau et al., 2003; King et al., 1993). We did not observe light-induced Fe(II) formation when illuminating chemically synthesized Fe(III) minerals (ferrihydrite) or biogenically produced Fe(III) oxyhydroxides that either contained freeze-dried bacterial cell residuals or were treated with H_2O_2 to remove microbial biomass (Fig. S2). The removal of biomass had no influence on the mineralogy of the biogenically formed Fe(III) oxyhydroxides as revealed by ^{57}Fe Mössbauer spectroscopy (Fig. S3 and Table S3). Illumination of different Fe(III)-organic complexes with higher photon flux and shorter light wavelengths generally led to faster and more complete formation of Fe(II) (Fig. 1). However, there were great differences in the overall extent of Fe(III) photoreduction by experiments with different organic ligands. While carboxylate groups, which are present in citrate, are able to undergo photochemical reactions when complexing Fe(III), hydroxamate and catecholate groups, which are abundant in many siderophores, are photostable when complexing Fe(III) (Barbeau et al., 2003). The overall extent of Fe(II) formation in light from complexes of Fe(III) with citrate, with siderophores from *Marinobacter* sp. TT1, or with siderophores from *Geobacter sulfurreducens,* showed clear differences (Fig. 1). While illumination of Fe(III)-citrate complexes with either a high VIS photon flux or UV light led to complete photoreduction of the Fe(III) within 96 h (Fig. 1 A, B), only 70% of Fe(III) complexed by siderophores of *Marinobacter* sp. was reduced within that time (UV 365 nm light; Fig. 1 D). Complexes of Fe(III) and siderophores of *Geobacter sulfurreducens* showed the lowest photo-susceptibility. Only by illumination with UV 365 nm light, more than 10% of the present Fe(III) could be reduced (Fig. 1 F). These differences in the overall photo-reactivity might originate from complexation of Fe(III) by different functional groups within the siderophores or from different stability constants of the Fe(III) complexes. Polycarboxylates, for instance, form strong complexes with Fe(III) and rapidly undergo photochemical reactions, but the composition of these carboxylic acids highly impacts their photosusceptibility (Abrahamson et al., 1994; Faust and Zepp, 1993; Kuma et al., 1995; Weller et al., 2013). The identity of the

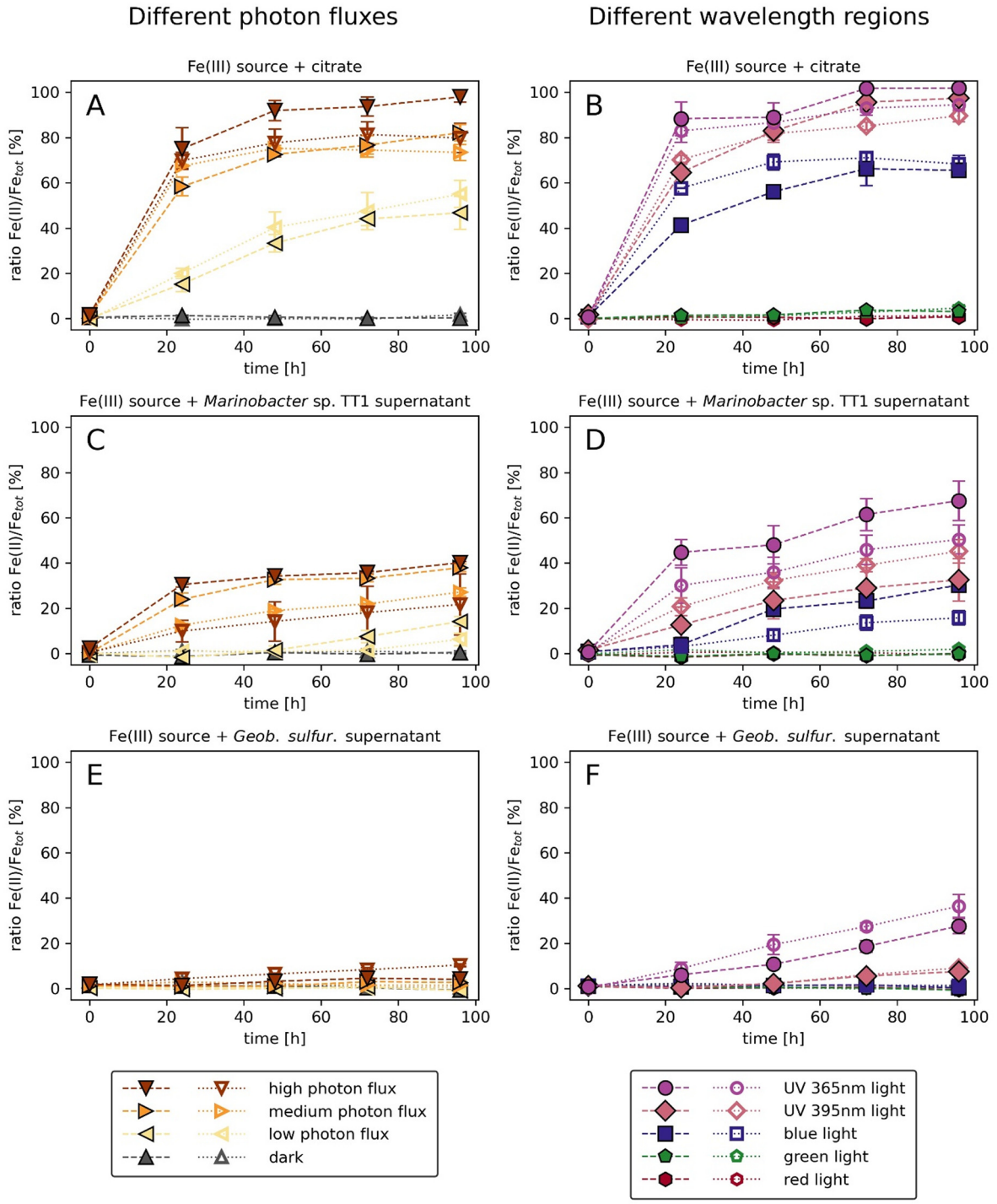

Fig. 1. Fe(II)/Fe_{tot} development over time under anoxic conditions during different illuminations (left: different photon fluxes of full VIS wavelength spectrum; right: different wavelength regions) with different Fe(III)-sources and organic complexing molecules. Closed symbols represent chemically synthesized ferrihydrite, open symbols represent biogenically formed Fe(III) oxyhydroxides. Organic complexing molecules are (A,B) citrate; (C,D) siderophores collected from supernatant of *Marinobacter* sp. TT1 culture, and (E,F) siderophores collected from supernatant of *Geobacter sulfurreducens* culture. Error bars show the standard deviation of triplicate experiments.

organic ligands present is crucial for the rates and extent of Fe(II) formation in light. Specifically, Fe(II) concentrations formed during 96 h illumination by a high photon flux of VIS light were more than twice (citrate vs. siderophores of *Marinobacter* sp.) or even ten times higher (citrate vs. siderophores of *Geobacter sulfurreducens*).

It remains unclear whether and how the identity of the Fe(III) source influences Fe(III) photoreduction efficiency. We found that the source of Fe (III) is of minor importance regarding the formation of photo-susceptible Fe(III)-organic complexes. Regardless of whether chemically synthesized ferrihydrite or biogenically formed Fe(III) oxyhydroxides are illuminated in the presence of organic ligands, Fe(II) could form to a similar extent depending on illumination conditions (Fig. 1). In general, slightly more Fe(II) formed in suspensions of organic ligands with abiogenic ferrihydrite compared to biogenically formed Fe(III) oxyhydroxides. The exact mineralogy of the biogenically formed Fe(III) oxyhydroxides is not known but they are presumably poorly crystalline (Kappler et al., 2021).

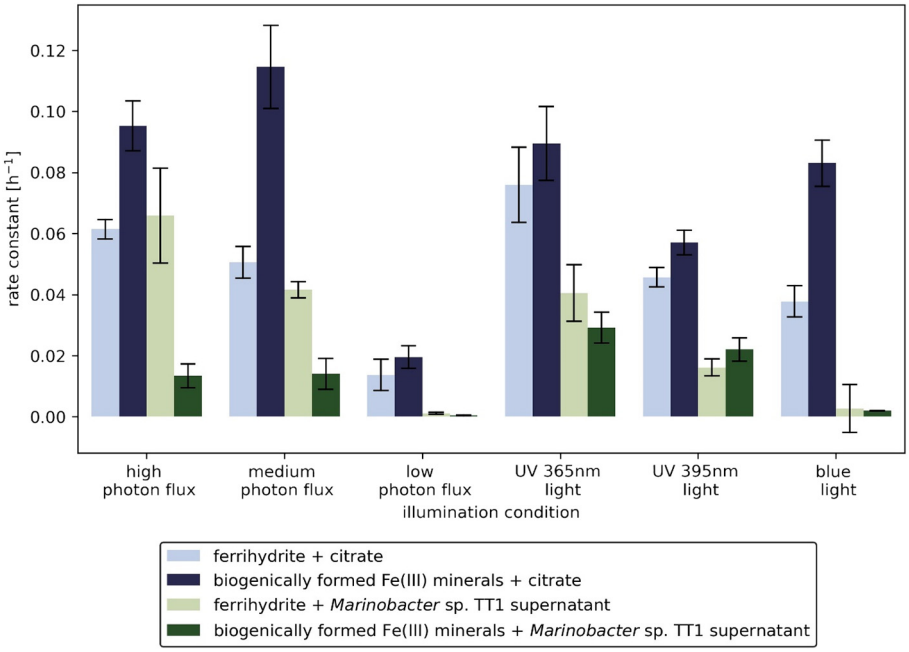

Fig. 2. Rate constants for Fe(III) photoreduction at anoxic conditions and different illumination conditions (Table S1) for chemically synthesized ferrihydrite and biogenically formed Fe(III) oxyhydroxides, either with citrate (blue bars) or with siderophores collected from supernatant of *Marinobacter* sp. TT1 culture (green bars). Error bars show the standard deviation of the fitted rate constants using Python. (For interpretation of the references to colour in this figure legend, the reader is referred to the web version of this article.)

3.3. Kinetics of Fe(III) photoreduction

Rate constants for Fe(III) photoreduction were obtained by curve fitting through Fe(II) concentration data measured in illuminated anoxic suspensions of ferrihydrite or biogenically produced Fe(III) oxyhydroxides with added citrate or siderophores from *Marinobacter* sp. TT1. Fitted curves, rate constants and goodness of the fit are presented in the Supporting Information (Fig. S4 and Table S4). The rate of Fe(III) photoreduction is influenced by the strength of the photon flux, the wavelength of illuminating light, and the identity of organic ligand and Fe(III) source. The following trends were observed: Using ferrihydrite as Fe(III) source, illumination with increasing photon flux or shorter wavelengths led to higher Fe(III) photoreduction rate constants of up to 0.075 h^{-1} (Fig. 2), independent of whether citrate or siderophores were present as organic ligands. Illumination of ferrihydrite-citrate suspensions with different wavelengths (UV 365 nm, UV 395 nm, blue light) led to 2–14 times higher Fe(III) photoreduction rate constants compared to suspensions of ferrihydrite and siderophores from *Marinobacter* sp. TT1.

If biogenic Fe(III) oxyhydroxides served as Fe(III) source, rate constants were either more than double compared to ferrihydrite (medium photon flux or blue light illumination) with citrate as organic ligand or only 20% (high photon flux illumination) with siderophores as organic ligand (Fig. 2). However, it has to be considered that Fe(III) photoreduction rate constants do not predict the final extent of Fe(III) photoreduction, i.e. if all available Fe(III) is photoreduced to Fe(II), but only the kinetics of Fe(II) formation. Thus, despite similar rate constants, illumination of ferrihydrite-siderophore suspensions with a high photon flux led to formation of less than 50% Fe(II) compared to when citrate was present as organic ligand (Fig. 1 A,C), indicating that presumably not all Fe(III) complexed by siderophores can be photoreduced. As Fe(III) photoreduction rates depend on several parameters, predictions of Fe(II) concentrations and comparison to other experimentally determined Fe(III) photoreduction rates are not straightforward, especially because most published rates were determined under fully oxic conditions, and compared to our study, at much lower Fe concentrations, in the presence of specific organic ligands and usually without separate consideration of different wavelength regions (King et al., 1995; Kuma et al., 1995; Pehkonen et al., 1993; Rijkenberg et al., 2004). For instance, King et al. (1995), calculated a Fe(III) photoreduction rate constant of 48 h^{-1} for wavelength- and volume-averaged incident light intensity for surface water. Other examples for such studies that had different (in some cases more specific) conditions than our study are the one by King et al. (1993), who found an apparent Fe(III) photoreduction rate of 0.06 h^{-1} in Argon-flushed NaCl solutions containing *p*-hydroxyphenylacetic acid, adjusted to pH 6.9 for a photon flux equivalent to midday summer sunlight, and the one by Kuma et al., (1995), who determined Fe(III) photoreduction rate constants ranging from 2.52–5.22 h^{-1} in seawater at pH 8.1 containing Fe(III)-glucaric acid complexes at different temperatures and light intensities.

3.4. Fe(III) photoreduction with concurrent Fe(II) oxidation

Molecular oxygen oxidizes Fe(II) chemically at rates that depend on pH as well as on O_2 and Fe(II) concentrations (Davison and Seed, 1983; Millero et al., 1987). In order to simulate relatively low O_2 conditions, prevalent in the upper millimeters of sediment (Laufer et al., 2016; Lueder et al., 2020a; Melton et al., 2014), 30% air (corresponding to ca. 6.3 vol% O_2, or dissolved O_2 concentrations of 85 μM at 20 °C) was added to the headspace of anoxic suspensions of ferrihydrite and citrate in which all Fe(III) had first been photoreduced to Fe(II). Fe(II) concentrations were followed during continuous illumination at different photon fluxes or wavelength regions (Table S1). In the dark, all Fe(II) was completely oxidized within 6–8 h (Fig. 3 A,B). Illumination with high, medium or low photon flux (VIS light), or with blue light, showed a similar trend in Fe(II) concentrations as incubation in the dark. The rate of Fe(II) oxidation, expressed as the drop in Fe(II) concentration with time was 170–250 μM h^{-1} within the first 30 min after aeration, decreasing to near-zero μM h^{-1} after 6 h of aeration (Fig. 3 C,D). Only illumination with UV light slowed down net Fe(II) oxidation for 1–1.5 h after aeration compared to all other illumination conditions or in dark (Fig. 3 C,D). The 395 and 365 nm UV light apparently produced Fe(II) by Fe(III) photoreduction at a sufficient rate to partly counterbalance the fast Fe(II) oxidation for a certain time. However, steady-state concentrations of Fe(II) were not reached, indicating decreasing Fe(III) photoreduction or increasing Fe(II) oxidation rates over time. This can be either due to the lack of available citrate forming fresh and photo-susceptible

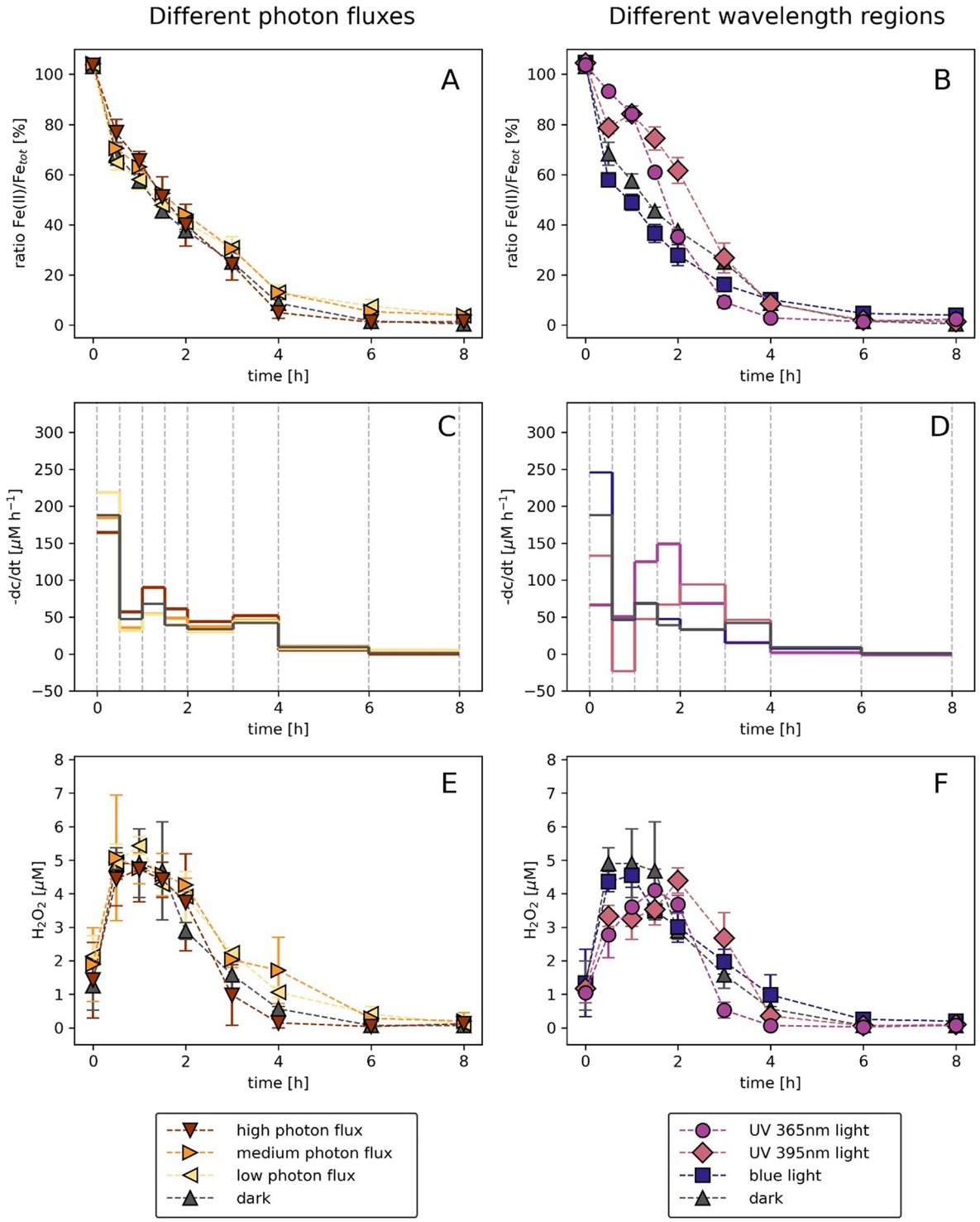

Fig. 3. Drop in Fe(II) concentration due to oxidation, expressed as the Fe(II)/Fe_{tot} ratio (A,B), net rates of Fe(II) oxidation over time (C,D), and H_2O_2 accumulation (E,F) over time of incubation under oxic conditions. The illumination conditions were, (left): different photon fluxes of full VIS wavelength spectrum 400–700 nm; (right): different wavelength regions. Dashed vertical lines in (C,D) indicate sampling time points. Error bars show the standard deviation of triplicate experiments.

Fe(III)-citrate complexes or due to increasing and fast heterogeneous Fe(II) oxidation after precipitation of Fe(III) minerals, which may serve as surface catalysts for further Fe(II) oxidation (Barnes et al., 2009; Tamura et al., 1976). Previous studies found that steady-state concentrations of Fe(II) formed within seconds to minutes upon irradiation in oxic seawater (Kuma et al., 1995; Laglera and Van Den Berg, 2007; Waite et al., 1995). However, those concentrations were in the picomolar to low micromolar range, which would not have been resolved by our quantification method (ferrozine assay (Stookey, 1970)). Fast heterogenous Fe(II) oxidation presumably plays a minor role at those low Fe concentrations due to less availability of Fe(III) mineral surfaces.

During the oxidation of Fe(II) by O_2, H_2O_2 formed within approx. 1 h of aeration at net concentrations of up to 5.5 μM, independent of wavelength of photon flux during illumination (Fig. 3 E,F). The H_2O_2 concentrations subsequently decreased, and after 6 h all H_2O_2 was consumed. As the H_2O_2 accumulation rate was largely similar during illumination with VIS

light and in the dark, and due to the lack of overlap between the absorption spectrum of citrate (Seraghni et al., 2012) and the wavelengths used in this study, H_2O_2 is not formed during photoreactions of organic matter (citrate) with O_2. It is rather formed during oxidation of either free, dissolved Fe(II), Fe(II) sorbed to Fe(III) minerals, or Fe(II)-citrate complexes according to Eqs. 1 and 2 or due to disproportionation of hydroperoxyl radicals ($HO•_2·$) formed by protonation of superoxide (Eqs. 3 and 4) (Rose and Waite, 2005):

$$Fe(II) + O_2 \rightarrow Fe(III) + O_2^{\cdot -} \quad (1)$$

$$Fe(II) + O_2^{\cdot -} + 2\,H^+ \rightarrow Fe(III) + H_2O_2 \quad (2)$$

$$O_2^{\cdot -} + H^+ \rightarrow HO_2^{\cdot} \quad (3)$$

$$HO_2^{\cdot} + HO_2^{\cdot} \rightarrow O_2 + H_2O_2 \quad (4)$$

Due to the high Fe concentrations used in our experiments compared to other studies, the produced H_2O_2 would expectedly be removed quickly by reaction with Fe(II) (eq. 5), eventually forming an Fe(IV)-oxo species (Buda et al., 2001) or hydroxyl radicals (·OH) (Zepp et al., 1992), which further oxidize Fe(II) (eq. 6) (Rose and Waite, 2002), and preventing further H_2O_2 accumulation.

$$Fe(II) + H_2O_2 \rightarrow Fe(III) + OH^- + \cdot OH \quad (5)$$

$$Fe(II) + \cdot OH \rightarrow Fe(III) + OH^- \quad (6)$$

Since H_2O_2 oxidizes Fe(II), the overall Fe(II) oxidation rate is enhanced compared to oxidation by O_2 only. As H_2O_2 accumulates, it can be assumed that other ROS, such as superoxide and hydroxyl radicals (Zepp et al., 1992), form as well (Eq. 1 & 5). Those ROS do not only oxidize Fe(II), but superoxide radicals can also reduce Fe(III), depending on presence and kind of organic complexation (Croot and Heller, 2012; Rose and Waite, 2002, 2005; Voelker and Sedlak, 1995). In UV light, Fe(II) concentrations decreased more slowly within the first hours after aeration compared to other illumination conditions (Fig. 3 B) or even appeared to slightly increase for a short time (UV 395 nm light, Fig. 3 B). Also, measured H_2O_2 concentrations under UV illumination are slightly lower than under other conditions during the first 1.5 h upon aeration (Fig. 3 F). As illumination of anoxic ferrihydrite-citrate suspensions with UV light and a high VIS photon flux led to similar rate of Fe(II) production (Fig. 1 A,B), an additional Fe(II) producing process besides LMCT reactions must take place during illumination with UV light in oxic conditions. Superoxide radicals can form by electron transfer from formed citrate radical ions upon LMCT reactions to O_2 (Feng et al., 2012; Ou et al., 2008).

The formed superoxide radicals apparently reduce Fe(III), either Fe(III) complexed with citrate or Fe(III) precipitated as Fe(III) (oxyhydr)oxide, and forms Fe(II) instead of oxidizing Fe(II) (eq. 2). By that process, H_2O_2 formation is retarded leading to less accumulation of H_2O_2. As Fe(III) photoreduction of Fe(III)-citrate causes decarboxylation of the citrate molecule (Bennett et al., 1982), the availability of citrate decreases over time, and less superoxide radicals and Fe(III)-citrate complexes can form. Fe(II) concentrations consequently decrease. Only during UV illumination does superoxide-mediated Fe(III) reduction apparently takes place to a significant extent, whereas other irradiation conditions do not lead to elevated Fe(II) concentrations compared to the dark control (Fig. 3 A,B). Concentrations of H_2O_2 were in the low micromolar range (0–7 μM, Fig. 3 E,F), which is approx. 10 times lower than found by Pehkonen et al. (1993) by experiments with amorphous $Fe(OH)_3$. However, those authors used lower Fe concentrations (130 μM) and high oxalate concentrations (6 mM), and they irradiated with UV light (320–370 nm) at acidic pH (pH = 3.2) under oxic conditions. As Fe(II) oxidation with O_2 and with H_2O_2 depends strongly on pH (Millero and Sotolongo, 1989), H_2O_2 can accumulate to higher concentrations before it is consumed by Fe(II) oxidation or by other reactions.

3.5. Importance of Fe(III)-organic complexation for Fe and H_2O_2 turnover

Organic complexation of Fe influences Fe redox kinetics. At circumneutral pH under oxic conditions, the solubility of Fe(III) is very low and it quickly precipitates as Fe(III) (oxyhydr)oxide. Organic complexation, however, can generally increase dissolved concentrations of Fe(III) (Kuma et al., 1996). Depending on the identity of organic ligands and their respective Fe(III)-complexing functional groups, these Fe(III)-organic complexes may undergo Fe(III) photoreduction upon irradiation (Barbeau et al., 2003). Organic complexation may also accelerate or retard the Fe(II) oxidation rate depending on source, molecular identity and functional characteristics of the organic ligands (Miles and Brezonik, 1981; Santana-Casiano et al., 2000; Theis and Singer, 1974) and thereby highly impact the persistence and availability of Fe(II). These differences are attributed to the relative affinity of Fe(II) or Fe(III) for complexation with different organic molecules (Lee et al., 2016), the relative stability of Fe(II)-ligand complexes (Krishnamurti and Huang, 1990), altered redox potentials of the Fe(II)/Fe(III) couple after organic complexation (Kappler et al., 2021; Rose and Waite, 2003a), or steric hindrances for the accessibility of O_2 to the complex (Kurimura et al., 1968; Rose and Waite, 2003a). However, it is still not completely understood how the origin or molecular composition of DOM impacts Fe(II) oxidation (Lee et al., 2016).

While Fe(II) was still available for 6 h after aeration (30% air) of a suspension of Fe(II) in the presence of citrate in our experiments (Fig. 3 A,B), all Fe(II) was oxidized within 3 h independent of illumination condition after similar aeration of anoxic $FeCl_2$ solutions without organic ligands (Fig. 4 A,B). Fe(II) oxidation during the first 30 min of aeration was slower for $FeCl_2$ alone compared to when citrate was present (Fig. 3 C,D and Fig. 4 C,D), but after 30 min the reaction accelerated to reach 300 μM h^{-1} (Fig. 4 C,D) after 1 h and then leveled off to 0 μM h^{-1} after 3 h of aeration. This Fe(II) development can be explained by purely homogeneous Fe(II) oxidation shortly after aeration, when dissolved Fe(II) is oxidized by dissolved O_2. Due to the lack of organic ligands, which could otherwise keep the produced Fe(III) in solution, Fe(III) (oxyhydr)oxides precipitated and served as surface catalyst for heterogeneous Fe(II) oxidation, which drastically accelerated the overall Fe(II) oxidation rate (Barnes et al., 2009; Tamura et al., 1976). Besides the catalytic effect of heterogeneous Fe(II) oxidation, complexation of Fe(II) by ligands can lead to faster oxidation rates compared to inorganic Fe(II) (Rose and Waite, 2003a). In the presence of siderophores of *Marinobacter* sp. TT1, Fe(II) oxidation was slightly accelerated (Fig. S5) compared to freely dissolved Fe(II) added as $FeCl_2$. As UV light (365 nm light) pre-illumination of anoxic suspensions of 300 μM ferrihydrite amended with siderophores of *Marinobacter* sp. TT1 only led to approx. 50% Fe(II) formation (Fig. S5 A), a corresponding amount of ferrihydrite (150 μM) was added to a $FeCl_2$ solution in a control setup before aeration to have a comparable amount of Fe(III) mineral surface. The addition of Fe(III) minerals led to fast Fe(II) oxidation, so that 0.5–1 h and 1.5 h after aeration, Fe(II) was completely oxidized in the presence (Fig. S5 A) or absence (Fig. S5 B) of siderophores of *Marinobacter* sp. TT1, respectively, independent of illumination with UV light (365 nm light) or incubation in dark.

The availability of organic ligands that can form photo-susceptible Fe(III)-organic complexes, as well as the ratio of ligands to Fe, are crucial for the redox state and fate of Fe and the accumulation of H_2O_2. Fig. 5 shows Fe(II) and H_2O_2 development in pre-illuminated (UV 365 nm light, anoxic) ferrihydrite-citrate suspensions over time, either with continuous UV illumination (365 nm light) or in the dark after aeration with 30% air. When 10 times more citrate than ferrihydrite (3 mM: 300 μM) was present, a stable ratio of approx. 0.75 Fe(II) to total Fe was established during UV illumination and lasted even 8 h upon aeration (Fig. 5 A). In suspensions at a citrate to ferrihydrite ratio of only 1:1 (300 μM: 300 μM), Fe(II) was completely oxidized after 4–6 h (Fig. 5 B). Thus, a high citrate concentration can balance Fe(III) photoreduction and Fe(II) oxidation by O_2 and other ROS by continuously forming fresh photo-susceptible Fe(III)-citrate complexes. Light-induced LMCT reaction or superoxide-mediated Fe(III) photoreduction forms Fe(II). Fe(II) oxidation continuously takes place,

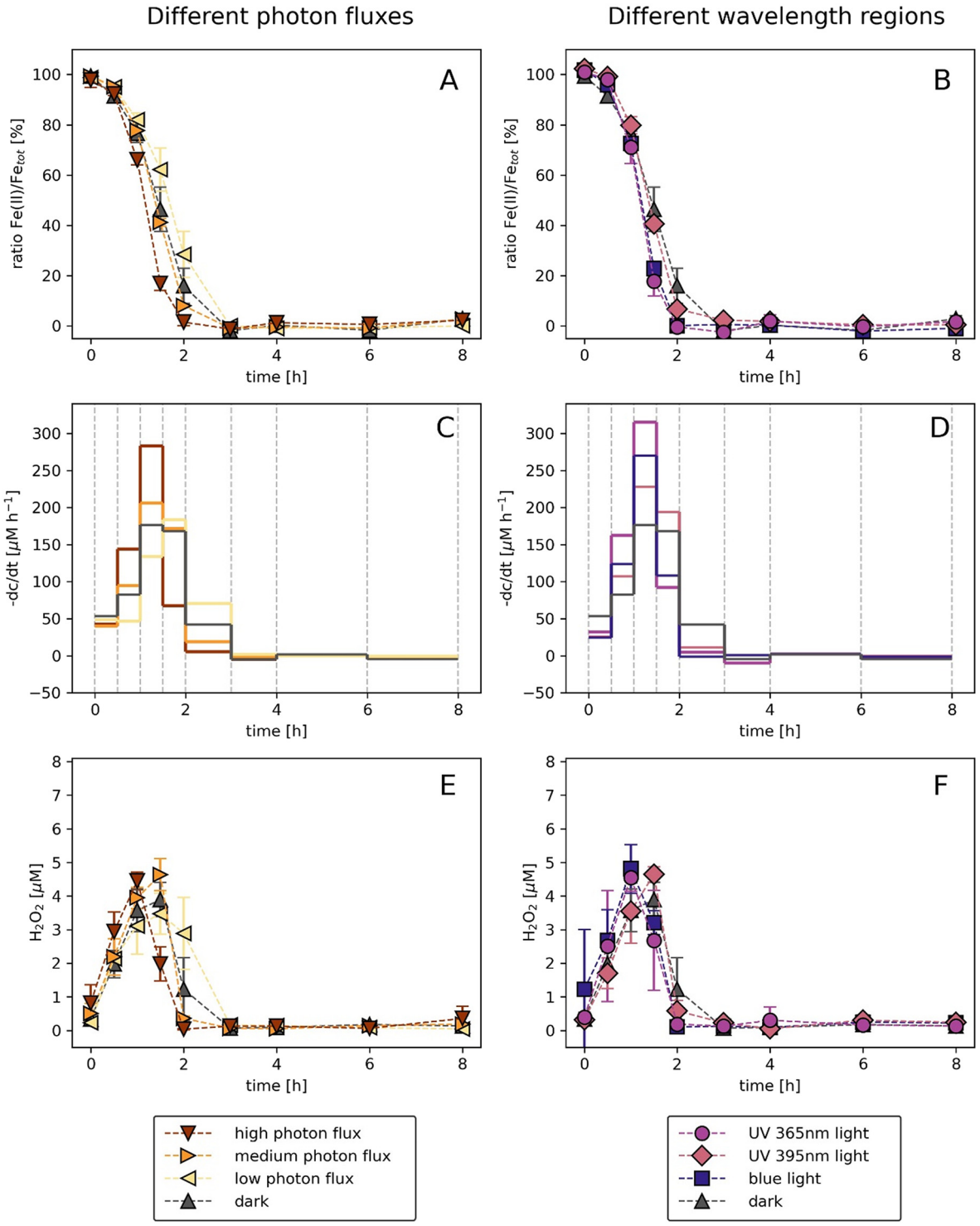

Fig. 4. Incubation experiments with $FeCl_2$ under oxic conditions. For further explanation, see Fig. 3 legend.

because after placing the UV irradiated suspension in the dark overnight (stopping photoreduction), all Fe(II) was oxidized. Therefore, light-induced cryptic Fe redox cycling took place leading to a steady state Fe(II) concentration (approx. 75% of total Fe). This steady-state concentration depends on the availability of Fe(III)-complexing ligands (Abrahamson et al., 1994). Others found decreasing steady-state concentrations of Fe(II) during extended irradiation of seawater and attributed this to photobleaching of DOM and consequently lower availability of organic ligands over time (Laglera and Van Den Berg, 2007; Rijkenberg et al., 2005; Rose and Waite, 2003b). The amount of Fe(III)-complexing organic ligands also affects Fe(II) oxidation kinetics in the dark. At 10-fold excess of citrate (Fig. 5 A), Fe(II) was completely oxidized after 2 h whereas at an Fe:citrate ratio of 1:1, it was only oxidized after 6 h (Fig. 5 B) during dark incubation.

Organic complexation also influenced H_2O_2 accumulation. During Fe(II) oxidation in the absence of organic ligands, H_2O_2 accumulated to a similar extent as in the presence of citrate and reached approx. 5 μM 1–1.5 h after aeration at all illumination conditions or in dark (Fig. 4 E,F). The H_2O_2 concentrations then decreased sharply and, when all Fe(II) was oxidized after 3 h, H_2O_2 could no longer be measured (Fig. 4 E,F). The observation that this accumulation and disappearance of H_2O_2 was independent of organic

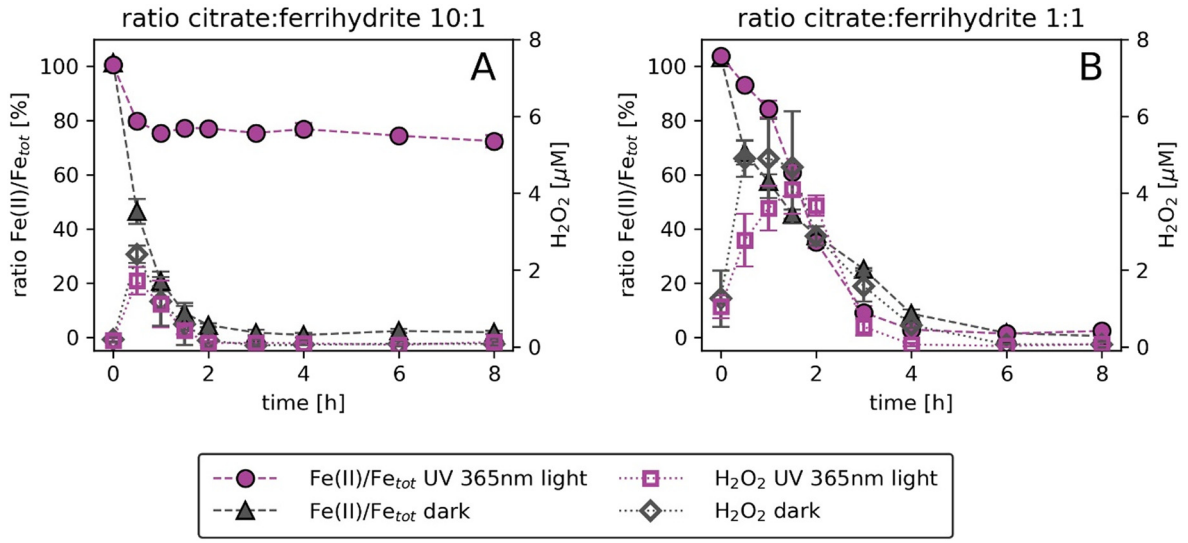

Fig. 5. Fe(II)/Fe_{tot} development and H_2O_2 accumulation over time of mixtures of ferrihydrite and citrate (pre-incubated in UV to photoreduce Fe(III)) in UV light or dark. (A) ratio citrate to ferrihydrite 10:1, (B) ratio citrate to ferrihydrite 1:1. Error bars show the standard deviation of triplicate experiments.

ligands or illumination conditions (Fig. 3 E,F and Fig. 4 E,F) indicates that H_2O_2 mainly formed by chemical Fe(II) oxidation. Light-induced reactions between organic ligands and O_2 apparently only play a minor role for controlling H_2O_2 dynamics at such high Fe(II) concentrations of several hundred μM. Interestingly, at high citrate concentrations (3 mM) less H_2O_2 accumulated (peaking at approx. 2 μM) compared to low citrate concentrations (300 μM), both during UV light (365 nm light) illumination and dark incubation (Fig. 5). During illumination with UV light, steady state concentrations of Fe(II) formed with continuous Fe(III) photoreduction and Fe(II) oxidation by O_2. Most superoxide radicals that are formed during Fe(II) oxidation by O_2 (eq. 1) presumably reduce Fe(III) (Rose and Waite, 2005), rather than oxidizing Fe(II) and forming H_2O_2 (eq. 2) or reacting with citrate. By that, less H_2O_2 is produced and accumulated.

3.6. Conclusions and environmental implications

In this study, well-defined systems with either abiogenic or biogenic Fe(III) oxyhydroxide minerals amended with Fe(III)-complexing organic ligands as well as Fe and O_2 concentrations relevant for sediments (Lueder et al., 2020a, 2020c; Schaedler et al., 2018) were illuminated with different photon fluxes and wavelength regions, which mimic light availability at different sediment depths. Although parameters such as wavelengths

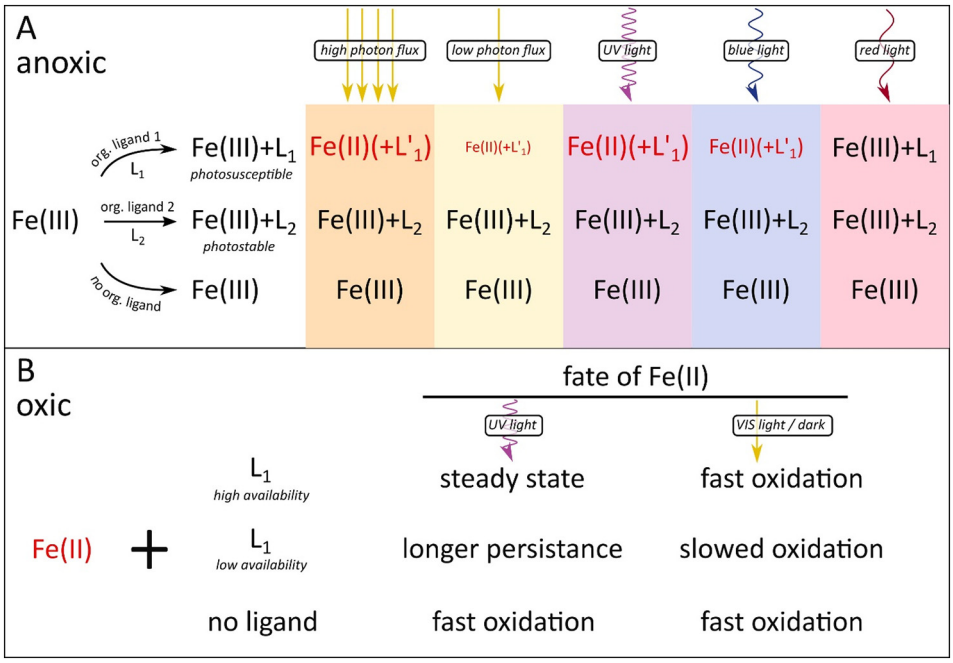

Fig. 6. Overview on parameters controlling Fe(III) photoreduction efficiency in (A) anoxic conditions with organic ligands forming photo-susceptible Fe(III)-ligand complexes (L_1, e.g. citrate), or photostable complexes (L_2) or in the absence of organic ligands. A high photon flux forms more Fe(II) (in red, eventually complexed by degraded organic ligand 1, L'_1) than low photon flux (smaller font size). More energy-rich light (UV) forms more Fe(II) than less energy-rich blue light (smaller font size). Red light is not able to photoreduce Fe(III) + L_1. In photostable Fe(III)-complexes (Fe(III) + L_2) or without organic ligands, Fe(III) is not reduced to Fe(II) at any illumination condition; and in (B) oxic conditions where photoproduced Fe(II) (in red) in the presence or absence of photo-susceptible ligands such as citrate lead to either steady state concentrations or different Fe(II) oxidation kinetics depending on illumination condition and availability of ligands. (For interpretation of the references to colour in this figure legend, the reader is referred to the web version of this article.)

distribution, photon flux, O_2 or Fe concentrations might vary in real sediments, our results can be extrapolated to Fe(III) photoreduction in sediments (Fig. 6). The amount of photoproduced Fe(II) is known to depend on light intensity, i.e. the photon flux (Kuma et al., 1995; Waite et al., 1995). However, we now show that an increase in photon flux does not necessarily lead to a proportional light-induced Fe(II) formation and that significant amounts of Fe(II) in the micromolar range were already formed at low light photon fluxes (Fig. 1 A).

Light penetrates only some millimeters into sediments due to strong absorption and scattering (Kühl et al., 1994; Lueder et al., 2020a, 2020b). The most effective wavelength range for light-induced Fe(II) production is UV light (Laglera and Van Den Berg, 2007; Rijkenberg et al., 2004, 2005), which is part of the natural sunlight spectrum. Despite being absorbed by chromophores in water (Johannessen et al., 2003) and also strongly absorbed in sediment, UV light can still be present in the upper hundreds of μm of sediment (Garcia-Pichel and Bebout, 1996) in case of a clear and shallow overlying water column. Here it can photoreduce Fe(III)-organic complexes, either by direct LMCT reactions or indirectly by superoxide radical formation upon interactions with DOM. Besides light, the concentration, availability and identity of organic ligands present in sediment pore waters are an important control parameter for Fe(III) photoreduction. We could now show that their available concentration changes the balance between Fe(III) reduction and Fe(II) oxidation in oxic sediment because their functional groups and ability to form photo-susceptible Fe(III)-organic complexes are crucial for Fe(III) photoreduction at circumneutral pH.

Light-induced cryptic iron cycling can lead to steady-state micromolar concentrations of Fe(II) in sediments, even in the presence of O_2 (Fig. 5 A) (Lueder et al., 2020a). Carboxylic acids, and specifically citrate as used in this study, as well as other organic ligands such as siderophores, humic substances or plant exudates are often found in the environment or in sediments (Borer and Hug, 2014; Fox and Comerford, 1990; Nebbioso and Piccolo, 2013; Saha et al., 2013). They form complexes with Fe(III) that are ubiquitously present, for instance as Fe(III) (oxyhydr)oxides (Kappler et al., 2021). Whether those Fe(III) (oxyhydr)oxides are biogenically or chemically formed, did not significantly change the efficiency of subsequent Fe(III) photoreduction. The availability and concentration of organic ligands in sediments not only control Fe(II) stability by impacting Fe(II) oxidation rates but also influence the formation and accumulation of H_2O_2 and potentially other ROS, such as hydroxyl radicals (White et al., 2003). Due to their high reactivity, they initiate Fe reactions and also influence other redox-sensitive element cycles (Hansel et al., 2015; Mopper and Zhou, 1990; Voelker et al., 2000).

Fe(III) photoreduction is an important Fe(II) source in light-influenced coastal freshwater and marine sediments, thereby changing the fluxes of Fe(II) (Lueder et al., 2020a, 2020c). Despite fast Fe(II) oxidation kinetics, Fe(III) photoreduction can lead to increased Fe(II) concentrations. The photo-produced Fe(II) is bioavailable (Johnson et al., 1994; Miller and Kester, 1994) and can serve as electron donor for, e.g. phototrophic Fe(II)-oxidizing bacteria (Peng et al., 2019), leading to light-driven Fe cycling. Compared to previous studies that analyzed parameters influencing Fe(III) photoreduction in the water column of freshwaters or the ocean, we could here determine experimentally how these parameters control Fe(III) photoreduction under sedimentary conditions. Our study helps to understand the extent and efficiency of Fe(III) photoreduction in sediments (Fig. 6) that maintain a constant formation and steady state concentrations of Fe(II), and to predict the Fe(II) availability in illuminated, organic-rich sediments.

CRediT authorship contribution statement

Ulf Lueder: Conceptualization, Investigation, Writing – original draft, Writing – review & editing, Visualization, Project administration. **Bo Barker Jørgensen:** Writing – original draft, Conceptualization, Visualization. **Markus Maisch:** Writing – original draft, Conceptualization. **Caroline Schmidt:** Writing – original draft, Conceptualization, Funding acquisition. **Andreas Kappler:** Resources, Writing – original draft, Writing – review & editing, Funding acquisition.

Declaration of competing interest

The authors declare that they have no known competing financial interests or personal relationships that could have appeared to influence the work reported in this paper.

Acknowledgements

The authors acknowledge infrastructural support by the Deutsche Forschungsgemeinschaft (DFG, German Research Foundation) under Germany's Excellence Strategy, cluster of Excellence EXC2124, project ID 390838134. We highly appreciate the help of L. Lueder for graphical design and thank Dr. A. Mellage for advice on kinetic calculations. This study was funded by the DFG to A.K. (grant KA 1736/57-1) and C.S. (grant SCHM2808/4-1). C.S. received additional funding from a Margarete von Wrangell fellowship (Ministry of Baden-Württemberg, Germany).

Appendix A. Supplementary data

Supporting information contains information on Fe(III) mineral synthesis and analysis, collection of organic ligands and rate calculations. Images and tables show experimental parameters and light spectra used for Fe(III) photoreduction experiments, ^{57}Fe Mössbauer spectra and fitting parameters of biogenically formed Fe(III) oxyhydroxides, fitted curves and modeled rate constants for Fe(II) development during anoxic Fe(III) photoreduction experiments and Fe(II)/Fe_{tot} development over time for mixtures of ferrihydrite with wither siderophores or $FeCl_2$, as well as for ferrihydrite or biogenically produced oxyhydroxides in the absence of organic ligands. Supplementary data to this article can be found online at doi: https://doi.org/10.1016/j.scitotenv.2021.152767.

References

Abrahamson, H.B., Rezvani, A.B., Brushmiller, J.G., 1994. Photochemical and spectroscopic studies of complexes, of iron(III) with citric acid and other carboxylic acids. Inorg. Chim. Acta 226, 117–127. https://doi.org/10.1016/0020-1693(94)04077-X.

Barbeau, K., 2006. Photochemistry of organic iron(III) complexing ligands in oceanic systems. Photochem. Photobiol. 82, 1505–1516. https://doi.org/10.1111/j.1751-1097.2006.tb09806.x.

Barbeau, K., Zhang, G., Live, D.H., Butler, A., 2002. Petrobactin, a photoreactive siderophore produced by the oil-degrading marine bacterium marinobacter hydrocarbonoclasticus. J. Am. Chem. Soc. 124, 378–379. https://doi.org/10.1021/ja0119088.

Barbeau, K., Rue, E.L., Trick, C.G., Bruland, K.W., Butler, A., 2003. Photochemical reactivity of siderophores produced by marine heterotrophic bacteria and cyanobacteria based on characteristic Fe(III) binding groups. Limnol. Oceanogr. 48, 1069–1078. https://doi.org/10.4319/lo.2003.48.3.1069.

Barnes, A., Sapsford, D.J., Dey, M., Williams, K.P., 2009. Heterogeneous Fe(II) oxidation and zeta potential. J. Geochem. Explor. 100, 192–198. https://doi.org/10.1016/j.gexplo.2008.06.001.

Bennett, J.H., Lee, E.H., Krizek, D.T., Olsen, R.A., Brown, J.C., 1982. Photochemical reduction of iron. II. Plant related factors. J. Plant Nutr. 5, 335–344. https://doi.org/10.1080/01904168209362962.

Borer, P., Hug, S.J., 2014. Photo-redox reactions of dicarboxylates and α-hydroxydicarboxylates at the surface of Fe(III)(hydr)oxides followed with in situ ATR-FTIR spectroscopy. J. Colloid Interface Sci. 416, 44–53. https://doi.org/10.1016/j.jcis.2013.10.030.

Borer, P., Sulzberger, B., Hug, S.J., Kraemer, S.M., Kretzschmar, R., 2009a. Photoreductive dissolution of iron(III) (hydr)oxides in the absence and presence of organic ligands: experimental studies and kinetic modeling. Environ. Sci. Technol. 43, 1864–1870. https://doi.org/10.1021/es801352k.

Borer, P., Sulzberger, B., Hug, S.J., Kraemer, S.M., Kretzschmar, R., 2009b. Wavelength-dependence of photoreductive dissolution of lepidocrocite (γ-FeOOH) in the absence and presence of the siderophore DFOB. Environ. Sci. Technol. 43, 1871–1876. https://doi.org/10.1021/es801353t.

Boyd, P.W., Ellwood, M.J., 2010. The biogeochemical cycle of iron in the ocean. Nat. Geosci. 3, 675–682. https://doi.org/10.1038/ngeo964.

Buda, F., Ensing, B., Gribnau, M.C.M., Baerends, E.J., 2001. DFT study of the active intermediate in the Fenton reaction. Chem. Eur. J. 7, 2775–2783. https://doi.org/10.1002/1521-3765(20010702)7:13<2775::AID-CHEM2775>3.0.CO;2-6.

Caccavo, F., Lonergan, D.J., Lovley, D.R., Davis, M., Stolz, J.F., McInerney, M.J., 1994. Geobacter sulfurreducens<(i> sp. nov., a hydrogen- and acetate-oxidizing dissimilatory metal-reducing microorganism. 60, 3752–3759. https://doi.org/10.1128/aem.60.10.3752-3759.1994.

Canfield, D.E., 1989. Reactive iron in marine sediments. Geochim. Cosmochim. Acta 53, 619–632. https://doi.org/10.1016/0016-7037(89)90005-7.

Cohn, C.A., Pak, A., Strongin, D., Schoonen, M.A., 2005. Quantifying hydrogen peroxide in iron-containing solutions using leuco crystal violet. Geochem. Trans. 6, 47. https://doi.org/10.1186/1467-4866-6-47.

Croot, P.L., Heller, M.I., 2012. The importance of kinetics and redox in the biogeochemical cycling of iron in the surface ocean. Front. Microbiol. https://doi.org/10.3389/fmicb.2012.00219.

Davison, W., Seed, G., 1983. The kinetics of the oxidation of ferrous iron in synthetic and natural waters. Geochim. Cosmochim. Acta 47, 67–79. https://doi.org/10.1016/0016-7037(83)90091-1.

Emmenegger, L., Schönenberger, R., Sigg, L., Sulzberger, B., 2001. Light-induced redox cycling of iron in circumneutral lakes. Limnol. Oceanogr. 46, 49–61. https://doi.org/10.4319/lo.2001.46.1.0049.

Faust, B.C., Zepp, R.G., 1993. Photochemistry of aqueous iron(III)-polycarboxylate complexes: roles in the chemistry of atmospheric andsurface waters. Environ. Sci. Technol. 27, 2517–2522. https://doi.org/10.1021/es00048a032.

Feng, X., Wang, Z., Chen, Y., Tao, T., Wu, F., Zuo, Y., 2012. Effect of Fe(III)/citrate concentrations and ratio on the photoproduction of hydroxyl radicals: application on the degradation of diphenhydramine. Ind. Eng. Chem. Res. 51, 7007–7012. https://doi.org/10.1021/ie300360p.

Fox, T.R., Comerford, N.B., 1990. Low-molecular-weight organic acids in selected forestsoils of the southeastern USA. Soil Sci. Soc. Am. J. 54, 1139–1144. https://doi.org/10.2136/sssaj1990.03615995005400040037x.

Garcia-Pichel, F., Bebout, B.M., 1996. Penetration of ultraviolet radiation into shallow water sediments: high exposure for photosynthetic communities. Mar. Ecol. Prog. Ser. 131, 257–262. https://doi.org/10.3354/meps131257.

Garg, S., Rose, A.L., Waite, T.D., 2011. Photochemical production of superoxide and hydrogen peroxide from natural organic matter. Geochim. Cosmochim. Acta 75, 4310–4320. https://doi.org/10.1016/j.gca.2011.05.014.

Garg, S., Jiang, C., Waite, T.D., 2018. Impact of pH on iron redox transformations in simulated freshwaters containing natural organic matter. Environ. Sci. Technol. 52, 13184–13194. https://doi.org/10.1021/acs.est.8b03855.

Garg, S., Xing, G., Waite, T.D., 2020. Influence of pH on the kinetics and mechanism of photoreductive dissolution of amorphous iron oxyhydroxide in the presence of natural organic matter: implications to iron bioavailability in surface waters. Environ. Sci. Technol. 54, 6771–6780. https://doi.org/10.1021/acs.est.0c01257.

Gledhill, M., Buck, K.N., 2012. The organic complexation of iron in the marine environment: a review. Front. Microbiol. https://doi.org/10.3389/fmicb.2012.00069.

Gorshkova, N.M., Ivanova, E.P., Sergeev, A.F., Zhukova, N.V., Alexeeva, Y., Wright, J.P., Nicolau, D.V., Mikhailov, V.V., Christen, R., 2003. Marinobacter excellens sp. nov., isolated from sediments of the Sea of Japan. Int. J. Syst. Evol. Microbiol. 53, 2073–2078. https://doi.org/10.1099/ijs.0.02693-0.

Gutierrez, T., Singleton, D.R., Berry, D., Yang, T., Aitken, M.D., Teske, A., 2013. Hydrocarbon-degrading bacteria enriched by the Deepwater Horizon oil spill identified by cultivation and DNA-SIP. ISME J. 7, 2091–2104. https://doi.org/10.1038/ismej.2013.98.

Hansel, C.M., Ferdelman, T.G., Tebo, B.M., 2015. Cryptic cross-linkages among biogeochemical cycles: novel insights from reactive intermediates. Elements 11, 409–414. https://doi.org/10.2113/gselements.11.6.409.

Hopwood, M.J., Statham, P.J., Skrabal, S.A., Willey, J.D., 2015. Dissolved iron(II) ligands in river and estuarine water. Mar. Chem. 173, 173–182. https://doi.org/10.1016/j.marchem.2014.11.004.

Johannessen, S.C., Miller, W.L., Cullen, J.J., 2003. Calculation of UV attenuation and colored dissolved organic matter absorption spectra from measurements of ocean color. J. Geophys. Res. Oceans 108. https://doi.org/10.1029/2000jc000514.

Johnson, K.S., Coale, K.H., Elrod, V.A., Tindale, N.W., 1994. Iron photochemistry in seawater from the equatorial Pacific. Mar. Chem. 46, 319–334. https://doi.org/10.1016/0304-4203(94)90029-9.

Kanzaki, Y., Murakami, T., 2013. Rate law of Fe(II) oxidation under low O2 conditions. Geochim. Cosmochim. Acta 123, 338–350. https://doi.org/10.1016/j.gca.2013.06.014.

Kappler, A., Bryce, C., Mansor, M., Lueder, U., Byrne, J.M., Swanner, E.D., 2021. An evolving view on biogeochemical cycling of iron. Nat. Rev. Microbiol. 19, 360–374. https://doi.org/10.1038/s41579-020-00502-7.

King, A.L., Barbeau, K.A., 2011. Dissolved iron and macronutrient distributions in the southern California Current System. J. Geophys. Res. Oceans 116. https://doi.org/10.1029/2010JC006324.

King, D.W., Lounsbury, H.A., Millero, F.J., 1995. Rates and mechanism of Fe(II) oxidation at nanomolar total iron concentrations. Environ. Sci. Technol. 29, 818–824. https://doi.org/10.1021/es00003a033.

King, W.D., Aldrich, R.A., Charnecki, S.E., 1993. Photochemical redox cycling of iron in NaCl solutions. Mar. Chem. 44, 105–120. https://doi.org/10.1016/0304-4203(93)90196-U.

Kraemer, S.M., 2004. Iron oxide dissolution and solubility in the presence of siderophores. Aquat. Sci. 66, 3–18. https://doi.org/10.1007/s00027-003-0690-5.

Krishnamurti, G.S.R., Huang, P.M., 1990. Kinetics of Fe(II) oxygenation and the nature of hydrolytic products as influenced by ligands. Sci. Geol. Mem. 195–204.

Krishnamurti, G.S.R., Huang, P.M., 1991. Influence of citrate on the kinetics of Fe(II) oxidation and the formation of iron oxyhydroxides. Clay Clay Miner. 39, 28–34. https://doi.org/10.1346/CCMN.1991.0390104.

Kühl, M., Lassen, C., Jørgensen, B.B., 1994. Light penetration and light intensity in sandy marine sediments measured with irradiance and scalar irradiance fiber-optic microprobes. Mar. Ecol. Prog. Ser. 105, 139–148. https://doi.org/10.3354/meps105139.

Kuma, K., Nakabayashi, S., Matsunaga, K., 1995. Photoreduction of Fe(III) by hydroxycarboxylic acids in seawater. Water Res. 29, 1559–1569. https://doi.org/10.1016/0043-1354(94)00289-J.

Kuma, K., Nishioka, J., Matsunaga, K., 1996. Controls on iron(III) hydroxide solubility in seawater: the influence of pH and natural organic chelators. Limnol. Oceanogr. 41, 396–407. https://doi.org/10.4319/lo.1996.41.3.0396.

Kurimura, Y., Ochiai, R., Matsuura, N., 1968. Oxygen oxidation of ferrous ions induced by chelation. Bull. Chem. Soc. Jpn. 41, 2234–2239. https://doi.org/10.1246/bcsj.41.2234.

Laglera, L.M., Van Den Berg, C.M.G., 2007. Wavelength dependence of the photochemical reduction of iron in arctic seawater. Environ. Sci. Technol. 41, 2296–2302. https://doi.org/10.1021/es061994h.

Laufer, K., Nordhoff, M., Røy, H., Schmidt, C., Behrens, S., Jørgensen, B.B., Kappler, A., 2016. Coexistence of microaerophilic, nitrate-reducing, and phototrophic Fe(II) oxidizers and Fe(III) reducers in coastal marine sediment. Appl. Environ. Microbiol. 82, 1433–1447. https://doi.org/10.1128/AEM.03527-15.

Lee, Y.P., Fujii, M., Terao, K., Kikuchi, T., Yoshimura, C., 2016. Effect of dissolved organic matter on Fe(II) oxidation in natural and engineered waters. Water Res. 103, 160–169. https://doi.org/10.1016/j.watres.2016.07.033.

Lee, Y.P., Fujii, M., Kikuchi, T., Terao, K., Yoshimura, C., 2017. Variation of iron redox kinetics and its relation with molecular composition of standard humic substances at circumneutral pH. PLoS One 12, e0176484. https://doi.org/10.1371/journal.pone.0176484.

Li, Y., Niu, J., Shang, E., Crittenden, J.C., 2015. Synergistic photogeneration of reactive oxygen species by dissolved organic matter and C60 in aqueous phase. Environ. Sci. Technol. 49, 965–973. https://doi.org/10.1021/es505089e.

Lueder, U., Jørgensen, B.B., Kappler, A., Schmidt, C., 2020a. Fe(III) photoreduction producing Feaq 2+ in oxic freshwater sediment. Environ. Sci. Technol. 54, 862–869. https://doi.org/10.1021/acs.est.9b05682.

Lueder, U., Jørgensen, B.B., Kappler, A., Schmidt, C., 2020b. Photochemistry of iron in aquatic environments. Environ Sci Process Impacts 22, 12–24. https://doi.org/10.1039/c9em00415g.

Lueder, U., Maisch, M., Laufer, K., Jørgensen, B.B., Kappler, A., Schmidt, C., 2020c. Influence of physical perturbation on Fe(II) supply in coastal marine sediments. Environ. Sci. Technol. 54, 3209–3218. https://doi.org/10.1021/acs.est.9b06278.

Luther, G.W., Shellenbarger, P.A., Brendel, P.J., 1996. Dissolved organic Fe(III) and Fe(II) complexes in salt marsh porewaters. Geochim. Cosmochim. Acta 60, 951–960. https://doi.org/10.1016/0016-7037(95)00444-0.

Marschner, H., Römheld, V., Horst, W.J., Martin, P., 1986. Root-induced changes in the rhizosphere: importance for the mineral nutrition of plants. Z. Pflanzenernähr. Bodenkd. 149, 441–456. https://doi.org/10.1002/jpln.19861490408.

Melton, E.D., Stief, P., Behrens, S., Kappler, A., Schmidt, C., 2014. High spatial resolution of distribution and interconnections between Fe- and N-redox processes in profundal lake sediments. Environ. Microbiol. 16, 3287–3303. https://doi.org/10.1111/1462-2920.12566.

Miles, C.J., Brezonik, P.L., 1981. Oxygen consumption in humic-colored waters by a photochemical ferrous-ferric catalytic cycle. Environ. Sci. Technol. 15, 1089–1095. https://doi.org/10.1021/es00091a010.

Miller, W.L., Kester, D., 1994. Photochemical iron reduction and iron bioavailability in seawater. J. Mar. Res. https://doi.org/10.1357/0022240943077136.

Miller, W.L., King, D.W., Lin, J., Kester, D.R., 1995. Photochemical redox cycling of iron in coastal seawater. Mar. Chem. 50, 63–77. https://doi.org/10.1016/0304-4203(95)00027-O.

Millero, F.J., Sotolongo, S., 1989. The oxidation of Fe(II) with H2O2 in seawater. Geochim. Cosmochim. Acta 53, 1867–1873. https://doi.org/10.1016/0016-7037(89)90307-4.

Millero, F.J., Sotolongo, S., Izaguirre, M., 1987. The oxidation kinetics of Fe(II) in seawater. Geochim. Cosmochim. Acta 51, 793–801. https://doi.org/10.1016/0016-7037(87)90093-7.

Mopper, K., Zhou, X., 1990. Hydroxyl radical photoproduction in the sea and its potential impact on marine processes. Science (80-.) 250, 661–664. https://doi.org/10.1126/science.250.4981.661.

Mostafa, S., Rosario-Ortiz, F.L., 2013. Singlet oxygen formation from wastewater organic matter. Environ. Sci. Technol. 47, 8179–8186. https://doi.org/10.1021/es401814s.

Mottola, H.A., Simpson, B.E., Gorin, G., 1970. Absorptiometric determination of hydrogen peroxide in submicrogram amounts with leuco crystal violet and peroxidase as catalyst. Anal. Chem. 42, 410–411. https://doi.org/10.1021/ac60285a017.

Nebbioso, A., Piccolo, A., 2013. Molecular characterization of dissolved organic matter (DOM): a critical review. Anal. Bioanal. Chem. 405, 109–124. https://doi.org/10.1007/s00216-012-6363-2.

Ou, X., Quan, X., Chen, S., Zhang, F., Zhao, Y., 2008. Photocatalytic reaction by Fe(III)-citrate complex and its effect on the photodegradation of atrazine in aqueous solution. J. Photochem. Photobiol. A Chem. 197, 382–388. https://doi.org/10.1016/j.jphotochem.2008.02.001.

Page, S.E., Logan, J.R., Cory, R.M., McNeill, K., 2014. Evidence for dissolved organic matter as the primary source and sink of photochemically produced hydroxyl radical in arctic surface waters. Environ Sci Process Impacts 16, 807–822. https://doi.org/10.1039/c3em00596h.

Pehkonen, S.O., Siefert, R., Erel, Y., Webb, S., Hoffmann, M.R., 1993. Photoreduction of iron oxyhydroxides in the presence of important atmospheric organic compounds. Environ. Sci. Technol. 27, 2056–2062. https://doi.org/10.1021/es00047a010.

Peng, C., Bryce, C., Sundman, A., Kappler, A., 2019. Cryptic cycling of complexes containing Fe(III) and organic matter by phototrophic Fe(II)-oxidizing bacteria. Appl. Environ. Microbiol. 85, e02826-18. https://doi.org/10.1128/AEM.02826-18.

Raddadi, N., Giacomucci, L., Totaro, G., Fava, F., 2017. Marinobacter sp. from marine sediments produce highly stable surface-active agents for combatting marine oil spills. Microb. Cell Factories 16, 186. https://doi.org/10.1186/s12934-017-0797-3.

Rich, H.W., Morel, F.M.M., 1990. Availability of well-defined iron colloids to the marine diatom Thalassiosira weissflogii. Limnol. Oceanogr. 35, 652–662. https://doi.org/10.4319/lo.1990.35.3.0652.

Rijkenberg, M.J.A., Gerringa, L.J.A., Neale, P.J., Timmermans, K.R., Buma, A.G.J., de Baar, H.J.W., 2004. UVA variability overrules UVB ozone depletion effects on the photoreduction of iron in the Southern Ocean. Geophys. Res. Lett. 31, 1–5. https://doi.org/10.1029/2004GL020829.

Rijkenberg, M.J.A., Fischer, A.C., Kroon, J.J., Gerringa, L.J.A., Timmermans, K.R., Wolterbeek, H.T., De Baar, H.J.W., 2005. The influence of UV irradiation on the photoreduction of iron in the Southern Ocean. Mar. Chem. 93, 119–129. https://doi.org/10.1016/j.marchem.2004.03.021.

Rijkenberg, M.J.A., Gerringa, L.J.A., Carolus, V.E., Velzeboer, I., de Baar, H.J.W., 2006. Enhancement and inhibition of iron photoreduction by individual ligands in open ocean seawater. Geochim. Cosmochim. Acta 70, 2790–2805. https://doi.org/10.1016/j.gca.2006.03.004.

Rose, A.L., Waite, T.D., 2002. Kinetic model for Fe(II) oxidation in seawater in the absence and presence of natural organic matter. Environ. Sci. Technol. 36, 433–444. https://doi.org/10.1021/es0109242.

Rose, A.L., Waite, T.D., 2003a. Effect of dissolved natural organic matter on the kinetics of ferrous iron oxygenation in seawater. Environ. Sci. Technol. 37, 4877–4886. https://doi.org/10.1021/es034152g.

Rose, A.L., Waite, T.D., 2003b. Predicting iron speciation in coastal waters from the kinetics of sunlight-mediated iron redox cycling. Aquat. Sci. 65, 375–383. https://doi.org/10.1007/s00027-003-0676-3.

Rose, A.L., Waite, T.D., 2005. Reduction of organically complexed ferric iron by superoxide in a simulated natural water. Environ. Sci. Technol. 39, 2645–2650. https://doi.org/10.1021/es048765k.

Saha, R., Saha, N., Donofrio, R.S., Bestervelt, L.L., 2013. Microbial siderophores: a mini review. J. Basic Microbiol. 53, 303–317. https://doi.org/10.1002/jobm.201100552.

Santana-Casiano, J.M., González-Dávila, M., Rodríguez, M.J., Millero, F.J., 2000. The effect of organic compounds in the oxidation kinetics of Fe(II). Mar. Chem. 70, 211–222. https://doi.org/10.1016/S0304-4203(00)00027-X.

Schaedler, F., Lockwood, C., Lueder, U., Glombitza, C., Kappler, A., Schmidt, C., 2018. Microbially mediated coupling of Fe and N cycles by nitrate-reducing Fe(II)-oxidizing bacteria in littoral freshwater sediments. Appl. Environ. Microbiol. 84, e02013-17. https://doi.org/10.1128/AEM.02013-17.

Scully, N.M., McQueen, D.J., Lean, D.R.S., 1996. Hydrogen peroxide formation: the interaction of ultraviolet radiation and dissolved organic carbon in lake waters along a 43–75°N gradient. Limnol. Oceanogr. 41, 540–548. https://doi.org/10.4319/lo.1996.41.3.0540.

Seraghni, N., Belattar, S., Mameri, Y., Debbache, N., Sehili, T., 2012. Fe(III)-citrate-complex-induced photooxidation of 3-methylphenol in aqueous solution. Int. J. Photoenergy 2012, 630425. https://doi.org/10.1155/2012/630425.

Singer, E., Webb, E.A., Nelson, W.C., Heidelberg, J.F., Ivanova, N., Pati, A., Edwards, K.J., 2011. Genomic potential of Marinobacter aquaeolei, a biogeochemical "Opportunitroph". Appl. Environ. Microbiol. 77, 2763–2771. https://doi.org/10.1128/AEM.01866-10.

Stookey, L.L., 1970. Ferrozine - a new spectrophotometric reagent for iron. Anal. Chem. 42, 779–781. https://doi.org/10.1021/ac60289a016.

Sulzberger, B., Suter, D., Siffert, C., Banwart, S., Stumm, W., 1989. Dissolution of Fe(III)(hydr)oxides in natural waters; laboratory assessment on the kinetics controlled by surface coordination. Mar. Chem. 28, 127–144. https://doi.org/10.1016/0304-4203(89)90191-6.

Tamura, H., Goto, K., Nagayama, M., 1976. The effect of ferric hydroxide on the oxygenation of ferrous ions in neutral solutions. Corros. Sci. 16, 197–207. https://doi.org/10.1016/0010-938X(76)90046-9.

Thamdrup, B., Fossing, H., Jørgensen, B.B., 1994. Manganese, iron and sulfur cycling in a coastal marine sediment, Aarhus bay, Denmark. Geochim. Cosmochim. Acta 58, 5115–5129. https://doi.org/10.1016/0016-7037(94)90298-4.

Theis, T.L., Singer, P.C., 1974. Complexation of iron(II) by organic matter and its effect on iron(II) oxygenation. Environ. Sci. Technol. 8, 569–573. https://doi.org/10.1021/es60091a008.

Voelker, B.M., Sedlak, D.L., 1995. Iron reduction by photoproduced superoxide in seawater. Mar. Chem. 50, 93–102. https://doi.org/10.1016/0304-4203(95)00029-Q.

Voelker, B.M., Morel, F.M.M., Sulzberger, B., 1997. Iron redox cycling in surface waters: effects of humic substances and light. Environ. Sci. Technol. 31, 1004–1011. https://doi.org/10.1021/es9604018.

Voelker, B.M., Sedlak, D.L., Zafiriou, O.C., 2000. Chemistry of superoxide radical in seawater: reactions with organic Cu complexes. Environ. Sci. Technol. 34, 1036–1042. https://doi.org/10.1021/es990545x.

Waite, T.D., Morel, F.M.M., 1984a. Photoreductive dissolution of colloidal iron oxides in natural waters. Environ. Sci. Technol. 18, 860–868. https://doi.org/10.1021/es00129a010.

Waite, T.D., Morel, F.M.M., 1984b. Photoreductive dissolution of colloidal iron oxide: effect of citrate. J. Colloid Interface Sci. 102, 121–137. https://doi.org/10.1016/0021-9797(84)90206-6.

Waite, T.D., Szymczak, R., Espey, Q.I., Furnas, M.J., 1995. Diel variations in iron speciation in northern Australian shelf waters. Mar. Chem. 50, 79–91. https://doi.org/10.1016/0304-4203(95)00028-P.

Weller, C., Horn, S., Herrmann, H., 2013. Photolysis of Fe(III) carboxylato complexes: Fe(II) quantum yields andreaction mechanisms. J. Photochem. Photobiol. A Chem. 268, 24–36. https://doi.org/10.1016/j.jphotochem.2013.06.022.

White, E.M., Vaughan, P.P., Zepp, R.G., 2003. Role of the photo-Fenton reaction in the production of hydroxyl radicals and photobleaching of colored dissolved organic matter in a coastal river of the southeastern United States. Aquat. Sci. 65, 402–414. https://doi.org/10.1007/s00027-003-0675-4.

Xing, G., Garg, S., David Waite, T., 2019. Is superoxide-mediated Fe(III) reduction important in sunlit surface waters? Environ. Sci. Technol. 53, 13179–13190. https://doi.org/10.1021/acs.est.9b04718.

Zepp, R.G., Faust, B.C., Jürg, H., 1992. Hydroxyl radical formation in aqueous reactions (pH 3–8) of iron(II) with hydrogen peroxide: the photo-fenton reaction. Environ. Sci. Technol. 26, 313–319. https://doi.org/10.1021/es00026a011.

Zhang, D., Yan, S., Song, W., 2014. Photochemically induced formation of reactive oxygen species (ROS) from effluent organic matter. Environ. Sci. Technol. 48, 12645–12653. https://doi.org/10.1021/es5028663.

Zhang, P., Yuan, S., 2017. Production of hydroxyl radicals from abiotic oxidation of pyrite by oxygen under circumneutral conditions in the presence of low-molecular-weight organic acids. Geochim. Cosmochim. Acta 218, 153–166. https://doi.org/10.1016/j.gca.2017.08.032.